Hindawi
International Journal of Antennas and Propagation
Volume 2023, Article ID 2024720, 10 pages
https://doi.org/10.1155/2023/2024720

Research Article

Parametric Model for Coaxial Cavity Filter with Combined KCCA and MLSSVR

Shengbiao Wu,[1,2] **Huaning Li**,[1] **and Xianpeng Chen**[1]

[1]*School of Mechanical and Electronic Engineering, East China University of Technology, Nanchang, Jiangxi, China*
[2]*Jiangxi Industry Technology Research Institute of Rehabilitation Assistance, Nanchang, Jiangxi, China*

Correspondence should be addressed to Shengbiao Wu; wsbdxm.hi@163.com

Received 7 March 2023; Revised 29 May 2023; Accepted 31 May 2023; Published 7 June 2023

Academic Editor: Giovanni Andrea Casula

Aiming at the problems of poor data effectiveness, low modeling accuracy, and weak generalization in the tuning process of microwave cavity filters, a parametric model for coaxial cavity filter using kernel canonical correlation analysis (KCCA) and multioutput least squares support vector regression (MLSSVR) is proposed in this study. First, the low-dimensional tuning data is mapped to the high-dimensional feature space by kernel canonical correlation analysis, and the nonlinear feature vectors are fused by the kernel function; second, the multioutput least squares support vector regression algorithm is used for parametric modeling to solve the problems of low accuracy and poor prediction performance; third, the support vector of the parameter model is optimized by the differential evolution whale algorithm (DWA) to improve the convergence and generalization ability of the model in actual tuning. Finally, the tuning experiments of two cavity filters with different topologies are carried out. The experimental results show that the proposed method has an obvious improvement in generalization performance and prediction accuracy compared with the traditional methods.

1. Introduction

The manufacture of coaxial cavity filters usually includes two steps: design and tuning. The design is mainly based on the electromagnetic simulation software, which produces approximate theoretical errors. In addition, the difference between processing tolerance and metal coating makes it difficult to achieve the physical size of the microwave cavity filter after production, and its output response cannot match the theoretical results. Therefore, tuning has become an indispensable link. To facilitate the tuning after processing, the tuning screws are usually installed on the real object to replace the resonant and coupling rods in the cavity. By constantly changing the direction and amplitude of the screws, the waveform of the output response can meet the requirements of the performance indicators.

In view of the complex dynamic characteristics such as nonlinearity and strong coupling in the tuning process of coaxial cavity filters, how to effectively use a large number of off-line and online data generated in the tuning process to establish a relationship model that can accurately reflect the tuning law is the focus of many scholars at home and abroad. At present, the relevant modeling methods mainly include feedback neural networks, fuzzy logic, and support vector regression algorithm. The research on neural network methods is concentrated on the basis of electromagnetic simulation software, such as the model between microwave element size and parameters [1], the tuning model between tuning element and return loss [2], and the model between reflection characteristic phase and center frequency [3]. However, the parameters in these models fluctuate greatly and are easily affected by the structure of microwave components, so it is difficult to extract the return loss and reflection characteristic phases. To reduce the amount of training data and shorten the modeling time, a high-precision microwave filter parameter prediction model using the adaptive learning neural network is proposed in [4]. It is applied to the optimization design of microwave filters. Although the neural network has strong nonlinear mapping ability, it has strict requirements for data quality. For the

cavity filter with insufficient field tuning data, the modeling accuracy has great limitations.

Faced with a complex tuning process, Miraftab first introduced engineers' experience in fuzzy rules into the tuning process of cavity filters [5]. This method uses experience and data fusion to establish the relationship model between coupling and tuning elements and is applied in low-order cavity filters. The drawback of this method is that it is difficult to apply to multiple cross-coupled cavity filters, and the process of designing fuzzy rules is extremely complex. Different from fuzzy algorithms, support vector regression modeling is a novel small-sample learning method with a solid theoretical foundation [6]. It has better generalization ability than the neural network when the number of samples is small. On the basis of previous research, multicore support vector regression based on parameter self-adjustment is used to model the tuning process of cavity filters [7]. However, faced with multi-input and multioutput data from cavity filters, the above method needs to solve the complex quadratic programming problem and should consider the coupling relationship between output variables. To improve the solving efficiency of multioutput systems, some studies using multicore machine learning have been proposed [8–12], which provides an important theoretical reference for the development of this study. Nonetheless, in industrial applications, the large-scale data collection and hyperparameter optimization time used for machine learning modeling often exceeds the tuning time. From a practical operational perspective, it is difficult to achieve.

To avoid these problems, parametric models based on vector field and machine learning were proposed in [13, 14], which provides a new idea for the modeling of the tuning process. However, with the increase in the order of the coaxial cavity filter, the input-output and action space dimensions of reinforcement learning increase sharply, resulting in an exponential growth of the value function network size and an increase in the training cost. In [15, 16], a parametric modeling method based on hybrid neural networks and deep learning has been proposed successively, but the data acquisition process of cavity filter in industrial applications is cumbersome, and the time of large-scale data acquisition will even exceed the tuning time. Therefore, from a practical point of view, these methods are difficult to implement. On the other hand, although SVR has obvious advantages in parametric modeling, the parameter identification of the algorithm itself relies too much on expert experience and laboratory experiments. Therefore, intelligent biomimetic algorithms such as the genetic algorithm (GA), particle swarm optimization algorithm (PSO), and genetic whale algorithm (GWA) are generally used to calculate parameters [17–19]. However, these algorithms also have the problem of easily falling into local optima and complex parameter calculations.

Given the aforementioned research analysis, the parametric model of coaxial cavity filters will encounter three challenges. (1) The difficulty of feature data fusion under different tuning modes and the impact of data validity on model accuracy. (2) Low modeling accuracy and weak generalization ability of parameterized models for multi-input multioutput tuning processes based on multivariate, strongly coupled, and nonlinear relational data. (3) Dealing with the computational efficiency and convergence speed of optimization algorithms in the solving process. The goal of this article is to provide a parametric model for cavity filter using kernel canonical correlation analysis and multioutput least squares support vector regression.

The contribution and novelty of this work includes three aspects: (i) the feature vectors under different modes of initial and fine tuning are fused by KCCA, which solves the problems of poor data validity and large input vector dimensionality of a single feature; (ii) the output coupling and complex computation process of quadratic programming in parameter modeling are avoided by combining the least squares method with the improved support vector regression; (iii) the differential evolution whale algorithm is used for model parameter identification, which improves the optimization speed and global search ability of the model. The rest of this study is organized as follows: Section 2 describes the theoretical synthesis of the cavity filter. Section 3 presents the principal component analysis of the raw data. Sections 4 and 5 mainly introduce the establishment of tuning model and parameter optimization. Section 6 shows the simulation results and analysis. The last section is the conclusion.

2. Theoretical Synthesis of Cavity Filter

2.1. Description of the Problem. The working process of this paper mainly includes data collection and kernel canonical correlation analysis, electromechanical characteristic modeling, and model parameter identification. First, collect the input and output data pairs (d, S) generated during the tuning process, where d denotes the screw tuning height and S denotes the corresponding output response; secondly, the coupling matrix is extracted from the scattering parameter (S-parameters) as mentioned in [20], and the characteristic parameters under different modes are fused through the kernel canonical correlation analysis technology. Build a data set for electromechanical characteristic modeling; finally, the electromechanical relationship model of the cavity filter based on multioutput support vector regression is established according to the collected data sets of input and output relationships. On this basis, the differential evolution whale algorithm is used to realize the adaptive identification of model parameters. The flow chart of the parametric model for the cavity filter is shown in Figure 1.

2.2. Mechanism and Characteristics of Cavity Filter. The produced coaxial cavity filter is difficult to achieve in physical size, and its output response cannot be consistent with the theoretical results. Generally, the cavity filter is equipped with tuning screws, and the output S-parameters can meet the performance requirements by changing the length of the tuning screws. The S-parameters have the following nonlinear relationship with the coupling matrix [21]:

$$\begin{aligned} S_{11} &= 1 + 2jR_1[sI - jR + M]^{-1}_{11}, \\ S_{21} &= -2j\sqrt{R_1R_2}[sI - jR + M]^{-1}_{n1}, \end{aligned} \tag{1}$$

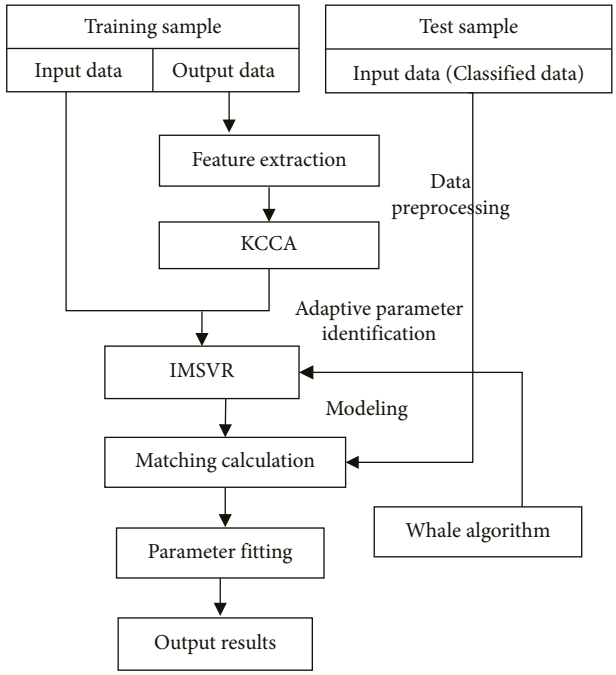

Figure 1: Flow chart of the parametric model for the cavity filter.

where R_1 and R_2 are the input and output port coupling, respectively. R denotes the diagonal matrix, I denotes the identity matrix. The coupling matrix (M) extracted from the S-parameter contains different feature information, such as diagonal elements, adjacent coupling elements, and cross-coupling elements, which are interrelated in different tuning stages. To reduce the redundant information in the tuning model, this study uses the KCCA multifeature fusion method to find the key information from the multidimensional features and convert the original extracted feature vector into a new low-dimensional vector.

3. Kernel Canonical Correlation Analysis

The tuning data of the cavity filter has serious nonlinear characteristics, especially for the cavity filter with initial tuning or multiple cross coupling. In addition, there is a strong coupling between the input variables, and it is difficult to describe the internal law of tuning with a single model. Therefore, data preprocessing and correlation analysis play a crucial role in modeling accuracy and generalization ability. The KCCA is a nonlinear data analysis algorithm, which transforms the nonlinear relationship of input space into the linear relationship of feature space through the kernel function and carries out correlation analysis in the new space. $\mathbf{P} = \{\mathbf{x} \mid \mathbf{x} \in \mathbf{R^p}\}$, $\mathbf{Q} = \{\mathbf{y} \mid \mathbf{y} \in \mathbf{R^q}\}$, $\mathbf{X} = (\mathbf{x_1}, \mathbf{x_2}, \ldots, \mathbf{x_n})$, and $\mathbf{Y} = (\mathbf{y_1}, \mathbf{y_2}, \ldots, \mathbf{y_n})$. The random variables in the observation space are transformed into the kernel function of the following high-dimensional space by implicit mapping [22].

$$\begin{cases} \varphi\colon x \in R^p \longrightarrow \varphi(x) \in H_x, \\ \phi\colon y \in R^q \longrightarrow \phi(y) \in H_y, \end{cases} \tag{2}$$

where R and H denote the observation space and high-dimensional feature space, respectively. $\varphi(x)$ and $\varphi(y)$ denote the implicit mappings of x and y from the observation space to high-dimensional feature space through kernel functions, respectively. $\varphi(\mathbf{x}) = (\varphi(\mathbf{x_1}), \varphi(\mathbf{x_2}), \ldots, \varphi(\mathbf{x_n}))$, $\phi(\mathbf{y}) = (\phi(\mathbf{y_1}), \phi(\mathbf{y_2}), \ldots, \phi(\mathbf{y_n}))$. The essence of the kernel function is equivalent to the mapping of input data from low-dimensional space to high-dimensional space, and its mathematical expression is as follows:

$$\begin{aligned} c &= \sum_{i=1}^{n} \varphi_i * \varphi_x(x_i), \\ d &= \sum_{i=1}^{n} \phi_i * \phi_y(y_i), \end{aligned} \tag{3}$$

where c and d denote the constant vectors of the high-dimensional space to be solved. $*$ denotes a multiplication sign. Using equation (3), the problem of solving high-dimensional space constant vectors c and d is transformed into the problem of solving low-dimensional space constant vectors φ_x and ϕ_y [23].

$$\begin{cases} X^* = c^{\mathrm{T}}\varphi_x(x) = \sum_{i=1}^{n} \varphi_i \langle \varphi_x(x_i), \varphi_x(x) \rangle, \\ Y^* = d^{\mathrm{T}}\phi_y(y) = \sum_{i=1}^{n} \phi_i \langle \phi_y(y_i), \phi_y(y) \rangle, \end{cases} \tag{4}$$

where X^* and Y^* denote the transformed characteristic components. T and $\langle \cdot \rangle$ denote the transpose and inner product, respectively. The core problem of KCCA is to solve the corresponding equations (3) and (4) when the correlation coefficient is the largest. The mathematical expression of the correlation coefficient is as follows [24]:

$$\rho = \mathrm{Corr}(X^*, Y^*) = \frac{\mathrm{Cov}(X^*, Y^*)}{\sqrt{\mathrm{Var}(X^*)}\sqrt{\mathrm{Var}(Y^*)}}, \tag{5}$$

where $\mathrm{Var}(\cdot)$ and $\mathrm{Cov}(\cdot)$ denote the variance matrix and covariance matrix, respectively. The variance and covariance of X^* and Y^* are calculated as follows:

$$\begin{cases} \mathrm{Var}(X^*) = c^{\mathrm{T}}\mathrm{var}(\varphi_x)c = \varphi_x^{\mathrm{T}}K(x,x)\varphi_x, \\ \mathrm{Var}(Y^*) = d^{\mathrm{T}}\mathrm{var}(\phi_y)d = \phi_y^{\mathrm{T}}K(y,y)\phi_y, \\ \mathrm{Cov}(X^*, Y^*) = c^{\mathrm{T}}\mathrm{cov}(\varphi_x, \phi_y)d = \varphi_x^{\mathrm{T}}K(x,y)\phi_y, \end{cases} \tag{6}$$

where $\mathbf{K}(\mathbf{x}, \mathbf{y}) = (\varphi_{\mathbf{x}}, \varphi_{\mathbf{y}})$, the following correlation coefficients can be obtained by substituting equations (5) into (6).

$$\rho = \frac{\varphi_x^{\mathrm{T}}K(x,y)\phi_y}{\sqrt{\varphi_x^{\mathrm{T}}K(x,x)\varphi_x * \phi_y^{\mathrm{T}}K(y,y)\phi_y}}. \tag{7}$$

The problem of solving the correlation coefficient is transformed into a constrained optimization problem, and its objective function and constraint conditions are as follows:

$$\begin{cases} \max\limits_{\varphi_x,\phi_y} \varphi_x^{\mathrm{T}} K(x,y)\phi_y, \\ \text{s.t.}\varphi_x^{\mathrm{T}} K(x,x)\varphi_x = \phi_y^{\mathrm{T}} K(y,y)\phi_y = 1. \end{cases} \tag{8}$$

The Lagrange multiplication is used to solve the above constrained extreme value problem, and the corresponding Lagrange equation is

$$\begin{aligned} L = \varphi_x^{\mathrm{T}} K(x,y)\phi_y - \frac{\rho_1}{2}\left(\varphi_x^{\mathrm{T}} K(x,x)\varphi_x - 1\right), \\ -\frac{\rho_2}{2}\left(\phi_y^{\mathrm{T}} K(y,y)\phi_y - 1\right), \end{aligned} \tag{9}$$

where ρ_1 and ρ_2 denote the Lagrange multiplier. Calculate the partial derivative of L with respect to φ_x and ϕ_y and make it zero. The following equations are obtained by deriving φ_x and ϕ_y, respectively.

$$\begin{cases} \dfrac{\partial L}{\partial \varphi_x} = K(x,y)\phi_y - \rho_1 K(x,x)\varphi_x = 0, \\ \dfrac{\partial L}{\partial \phi_y} = K(y,x)\varphi_x - \rho_2 K(x,x)\phi_y = 0, \end{cases} \tag{10}$$

where $\rho_1 = \rho_2 = \lambda$, the solution of KCCA problem is equivalent to solving the eigenvector problem corresponding to the following generalized eigenequation:

$$\begin{bmatrix} 0 & K_x K_y \\ K_y K_x & 0 \end{bmatrix} \begin{bmatrix} \varphi_x \\ \phi_y \end{bmatrix} = \lambda \begin{bmatrix} K_x K_x & 0 \\ 0 & K_y K_y \end{bmatrix} \begin{bmatrix} \varphi_x \\ \phi_y \end{bmatrix}, \tag{11}$$

where $\mathbf{K_x} = \varphi_{\mathbf{x}}^{\mathrm{T}}\varphi_{\mathbf{x}}$, $\mathbf{K_y} = \phi_{\mathbf{y}}^{\mathrm{T}\phi_{\mathbf{y}}}$, and $\varphi_{\mathbf{x}}$ and $\phi_{\mathbf{y}}$ denote the eigenvectors to be solved. By solving the above equation, $\varphi_{\mathbf{x}}$, $\phi_{\mathbf{y}}$, and the correlation coefficient ρ can be calculated.

4. Parametric Modeling

The traditional multioutput regression problem is usually solved by transforming the multidimensional output into one dimensional output, which often ignores the correlation between variables, to reduce the accuracy of the model. To solve this problem and fully consider the correlation of output components, this study improves the loss function of the original algorithm and proposes a parametric modeling strategy combining KCCA and MLSSVR.

4.1. Support Vector Regression. The essence of support vector regression is to map the input space to the high-dimensional space through nonlinear mapping and perform linear regression through the estimation function in the high-dimensional space. In this study, select the training set $(\mathbf{x_i}, \mathbf{y_i}) \in \mathbf{R^p} \times \mathbf{R^q}$ of n group sample data, in which the input variable $\mathbf{x_i} = (\mathbf{x_{i1}}, \mathbf{x_{i2}}, \cdots \mathbf{x_{ip}})^{\mathrm{T}}$ and the output variable $\mathbf{y_i} = (\mathbf{y_{i1}}, \mathbf{y_{i2}}, \cdots \mathbf{y_{iq}})^{\mathrm{T}}$. This research improves the insensitive loss function in the traditional single-output function regression algorithm, using the loss function on the hypersphere instead of the loss function on the hypercube. The improved loss function is as follows [25]:

$$L\left(\left\|e_i\right\|\right) = \begin{cases} 0 & \left\|e_i\right\| < \varepsilon, \\ \left(\left\|e_i\right\| - \varepsilon\right)^2 & \left\|e_i\right\| \geq \varepsilon, \end{cases} \tag{12}$$

where $\|e_i\| = \sqrt{e_i^T e_i}$, $e_i = y_i - \varphi^{\mathrm{T}}(x_i)w - b^{\mathrm{T}}$, and ε denotes the width of the neutral zone, which is the tolerance for errors, φ denotes a nonlinear mapping function, $\mathbf{b} = [\mathbf{b_1}\ \mathbf{b_2} \cdots \mathbf{b_n}]$, $w = [w_1\ w_2 \cdots w_n]$, i denotes the number of input samples, and q denotes the dimension of the output variable. The improved function takes the fitting error of each component into account, which can not only achieve the goal of overall optimization, but also weaken the noise.

4.2. Multioutput Least Squares Support Vector Regression. Different from support vector machines, LS-SVR usually rewrites the primary loss function into a quadratic loss function and changes the inequality constraints into equality constraints, which avoids the complex calculation of solving quadratic programming problems and improves the efficiency of optimization. However, the traditional LS-SVR algorithm is only applicable to the regression modeling of single-output systems. When faced with multioutput nonlinear systems, the single-output systems are usually simply combined, thus ignoring the potential correlation information between output variables. In view of this, this study improved the objective function and constraint equation and used the absolute error to describe the overall error of the sample, thus establishing a multioutput regression model. The parametric model structure is shown in Figure 2, where u, v, and w denote the resonant cavity self-coupling, adjacent cavity coupling, and cross coupling variables, respectively. g, s, and t denote the number of corresponding variables. The model has a simple structure and is easy to calculate. The new eigenvector x_i in the parametric model is mapped to the high-dimensional space $\varphi(x_i)$, and then the linear modeling is realized in the new feature space [26].

$$y_i = \sum_{i=1}^{n} \alpha_i \langle \varphi(x), \varphi(x_i) \rangle + b_i, \tag{13}$$

where $\mathbf{K}(\mathbf{x}, \mathbf{x_i}) = \langle \varphi(\mathbf{x}), \varphi(\mathbf{x_i}) \rangle$ denotes the nonlinear mapping. In this study, the least squares method is introduced to change the inequality constraint in traditional support vector regression into an equality constraint, and the square term of error is used as the experience loss of the training set. Finally, the quadratic programming problem is transformed into solving linear equations, which improves the calculation speed and convergence accuracy of the algorithm. The values of w and b are obtained through the following optimization and constraint functions [27]:

$$\begin{aligned} &\min J = \frac{1}{2}\sum_{r=1}^{q} \left\|w_r\right\|^2 + \frac{C}{2}\sum_{i=1}^{n}\sum_{r=1}^{q} e_{ir}^2 + c_0 \sum_{i=1}^{n} E_{ir}, \\ &\text{s.t.} \begin{cases} e_{ir} = y_{ir} - w_r \varphi_r^{\mathrm{T}}(x_i) - b_{ir}, \\ E_{ir} = \left\|y_{ir} - f(x_{ir})\right\|^2, \end{cases} \end{aligned} \tag{14}$$

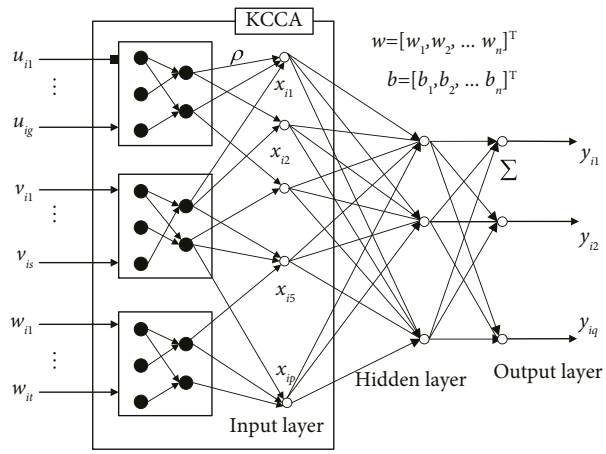

Figure 2: Parametric model structure of coaxial cavity filter.

where $\mathbf{x_i} = [\mathbf{x_{i1}}\,\mathbf{x_{i2}}\cdots\mathbf{x_{ip}}]^{\mathrm{T}}$, and $\mathbf{y_i} = [\mathbf{y_{i1}}\,\mathbf{y_{i2}}\cdots\mathbf{y_{iq}}]^{\mathrm{T}}$ denote the input and output variables. $\mathbf{w_i} = [\mathbf{w_1}\,\mathbf{w_2}\cdots\mathbf{w_n}]^{\mathrm{T}} \in \mathbf{R^{n\times q}}$ denote the output weight, $\mathbf{b_i} = [\mathbf{b_1}\,\mathbf{b_2}\cdots\mathbf{b_n}]^{\mathrm{T}} \in \mathbf{R^n}$ denotes the bias coefficient vector, $\varphi(\mathbf{x_i}) = [\varphi_1(\mathbf{x_i})\,\varphi_2(\mathbf{x_i})\cdots\varphi_{\mathbf{n}}(\mathbf{x_i})]^{\mathrm{T}}$ denotes the input mapping function, c_0 denotes the penalty coefficient of the overall error of the sample, C denotes the j-th dimension output error of the i-th sample, e_{ir} denotes the j-dimensional output error of the i-th sample, and E_i denotes the overall fitting error. The objective function and constraints are transformed into the following Lagrange function:

$$L = \frac{1}{2}\sum_{r=1}^{q}\|w_r\|^2 + \frac{C}{2}\sum_{i=1}^{n}\sum_{r=1}^{q}e_{ir}^2 + c_0\sum_{i=1}^{n}E_{ir}^2 - \sum_{i=1}^{n}\sum_{r=1}^{q}\alpha_{ir}\left(y_{ir} - w_r^{\mathrm{T}}\varphi(x_i) - b_{ir} - e_{ir}\right), \tag{15}$$

where $\alpha = [\alpha_1\,\alpha_2\cdots\alpha_{\mathbf{q}}]$ and $\beta = [\beta_1\,\beta_2\cdots\beta_{\mathbf{q}}]$ denote Lagrange factor. Use equation (3) to calculate the partial derivatives of w_r, b_r, e_{ir}, and α_{ir}, respectively, and obtain the following expression with KKT condition:

$$\begin{cases} \dfrac{\partial L}{\partial w_r} = 0 \longrightarrow \omega_r = \displaystyle\sum_{i=1}^{n}\alpha_{ir}\varphi(x_i), \\ \dfrac{\partial L}{\partial b_{ir}} = 0 \longrightarrow \displaystyle\sum_{i=1}^{n}\alpha_{ir} = 0, \\ \dfrac{\partial L}{\partial e_{ir}} = 0 \longrightarrow C\cdot e_{ir} = \alpha_{ir}, \\ \dfrac{\partial L}{\partial \alpha_{ir}} = 0 \longrightarrow y_{ir} - w_r^{\mathrm{T}\varphi}(x_i) - b_{ir} - e_{ir} = 0. \end{cases} \tag{16}$$

By eliminating w_r and e_{ir}. The solution of the optimization problem can be transformed into the solution of the following linear equations:

$$\begin{bmatrix} 0 & I^T \\ I & k(x,x_r) + c_0^{-1} \end{bmatrix}\begin{bmatrix} b_{ir} \\ \alpha_{ir} \end{bmatrix} = \begin{bmatrix} 0 \\ y_r + c_0\cdot\dfrac{\hbar_r}{C} \end{bmatrix}, \tag{17}$$

where $\mathbf{I}$ denotes the unit matrix, $\mathbf{k}(\mathbf{x},\mathbf{x_r}) = \varphi^{\mathrm{T}}(\mathbf{x})\varphi(\mathbf{x_r})$. When the output error of the r-th dimension is greater than or equal to zero, $\hbar_r = 1$. The values of the variables b_r and w_r are obtained by solving the above linear equations, and the regression function of the output of the r-dimension is as follows:

$$f_r(x) = \sum_{i=1}^{n}\alpha_{ir}k_r(x,x_r) + b_{ir}. \tag{18}$$

The Gaussian radial basis function has good ability to handle complex nonlinear relationships between sample inputs and output. It requires fewer parameters to be determined and has high computational efficiency. Therefore, the kernel function used in this study is the Gaussian radial basis function:

$$k(x,x_r) = \exp\left(\frac{-\|x - x_r\|}{2\sigma^2}\right), \tag{19}$$

where σ denotes the kernel width parameter, which reflects the size of the training data sample space range. When its value is large, the space range is small. When the number of support vectors is large and the regression parameters have been calculated, the kernel method may suffer from the curse of dimensionality. To effectively utilize all sample information, a sparsization method based on singularity criteria is used to continuously update the sample subset. This subset effectively reduces the redundant information of input samples while maximizing the coverage of input sample information, thus significantly reducing the solution size. The main steps include (1) initialize an empty sample set D_0, and when obtaining the first sample vector x_1, make $D_1 = x_1$; (2) when the number of samples is greater than 1, calculate the minimum distance $\gamma = \min_{x_v\in D_i}\|x_i - x_v\|$ between the new sample x_i and the current sample set; (3) when the minimum distance is less than a preset threshold δ_1, (x_i, y_i) is not added to D_i, otherwise the prediction error e_i is calculated; and (4) when $|e_i|$ is greater than the preset threshold δ_2, add (x_i, y_i) to D_i and update D_i to D_{i+1}, otherwise proceed to (2). The thresholds δ_1 and δ_2 are used to control the accuracy and scale of the solution. Increasing δ_1 and δ_2 is beneficial for reducing the size of sample set D, but it will lead to a decrease in the performance of the beamformer. This article takes δ_1 as 0.1 of the kernel radius and δ_2 as the root mean squares value of the average steady-state mean square error, which can achieve high computational accuracy on a smaller scale. The steps to establish the parametric model of the cavity filter using MLSSVR algorithm are as follows:

Step 1: Set the initial value of C, σ, and c_0. Based on the collected sample dataset, the MLSSVR algorithm is used to establish the regression function of the multi-input and output tuning system for the cavity filter.

Step 2: Substitute the input and output matrices and relevant parameters of training samples into the sub-function. Use the established initial regression function to detect the test sample data and calculate the test error e_{ir};

Step 3: For any r-th dimension output, the value of $\hbar_r$ is determined according to e_{ir};

Step 4: According to the calculated α_{ir} and b_r, the regression function of the cavity filter multi-input and output tuning system is established. The work flow chart of the improved whale algorithm is shown in Figure 3.

5. Parameters Identification

The forecast accuracy of MLSSVR is mainly affected by the kernel function parameter σ, the penalty factor C and c_0, where the value of the penalty factor corresponds to the empirical risk generated by the training samples. If the penalty factor is too small, the punishment for exceeding the insensitive band in the sample is too small, and the training error is too large. On the contrary, if the penalty factor is too large, the error penalty will be too large, while the model structure restriction will be reduced, resulting in the model being too complex; the kernel function parameters can reflect the distribution of sample data in high-dimensional feature space information.

5.1. Differential Evolution Whale Algorithm. DWA is a heuristic-intelligent algorithm that imitates the behavior of whale predation. Compared with the traditional optimization algorithm, it has the advantages of less control parameters, a simple implementation, and high flexibility. DWA imitates the whale's predation method, which mainly includes three stages hunting predation, bubble net predation, and free search. The position of each individual represents the potential solution, and the global optimal solution is obtained by constantly updating the position of the whale.

Shrink Surround: Since there is no prior knowledge of the global optimal solution of the search space before solving the optimization problem, a population of individuals is randomly selected as the target for predatory activities, and other whale individuals in the population are surrounded by the optimal individuals. The position update equation is as follows [28]:

$$\begin{cases} x_i(k+1) = x_i^*(k) + \overrightarrow{F}(k) \cdot d', \\ d' = \overrightarrow{J}(k) \cdot x_i^*(k) - x_i(k), \end{cases} \tag{20}$$

where $x_i(k+1)$ denotes the position of the i-th whale at iteration k. $\overrightarrow{F}(k)$ and $\overrightarrow{J}(k)$ denote the coefficient vector, and $\overrightarrow{F}(k) = 2\delta * r\text{and}(\cdot) - \delta$, $\overrightarrow{J}(k) = 2r\text{and}(\cdot)$, δ denotes the convergence factor of linear descent. $r\text{and}(\cdot)$ denotes the random number in $[0, 1]$. In the process of bubble net predation, the position update between whale and prey is expressed by the following logarithmic spiral equation [29]:

$$\begin{cases} x_i(k+1) = d_i' e^{\vartheta l} \cos(2\pi l) + x^*(k), \\ d_i' = \left| x^*(k) - x_i(k+1) \right|, \end{cases} \tag{21}$$

where d_i' denotes the distance between the search individual and the current optimal solution, ϑ denotes the spiral shape parameter, l denotes a random number uniformly distributed in $[-1, 1]$, and $x^*(k)$ denotes the current best position vector. The algorithm can choose the predation behavior by setting the probability γ of the predation mechanism. The whale's position update equation is as follows [30]:

$$x_i(k+1) = \begin{cases} x_i(k+1) - \overrightarrow{F}(k) \cdot d(k) \, \gamma \in [0, 0.5), \\ d_i' e^{\vartheta l} \cos(2\pi l) + x^*(k) \, \gamma \in [0.5, 1), \end{cases} \tag{22}$$

where $|\gamma| < 1$, each whale is in the phase of gradually surrounding the current optimal solution. To ensure that all whales can search completely in the solution space, the distance between whales in the whale algorithm is used to update the position to achieve the purpose of random search. Therefore, when $|\gamma| \geq 1$, the search experience will swim toward the random whale.

$$\begin{cases} x_i(k+1) = x_r(k) + \overrightarrow{F}(k) \cdot d'', \\ d'' = \overrightarrow{J}(k) \cdot x_r(k) - x_i(k), \end{cases} \tag{23}$$

where $x_r(k)$ denotes the position of the current random individual. d'' denotes the distance between the current search individual and the optimal solution. To increase the diversity of the population, the differential evolution is introduced in the process of population position updating, which avoids the premature phenomenon brought by the local optimal solution. The location updating formula is as follows:

$$x_i(k+1) = \tau \cdot \left(x^* - x_i(k)\right) + \tau \cdot \left(x_r(k) - x_i(k)\right), \tag{24}$$

where x^* and $x_r(k)$ denote the optimal individual position and the random individual, respectively, k denotes iterations and τ is a random number in [0 1]. This study combines the powerful exploration capabilities of differential evolution algorithm with the whale algorithm to enhance the development space of the whale algorithm. First, the whale algorithm is used to preprocess the position of the individual population and generate an initial population. Then, the differential evolution algorithm is used to cross-select the generated population to achieve population update iteration. The algorithm process is shown in Table 1.

To prevent over- and underfitting of the model, the insensitivity coefficient is given empirically in this study. Select the following sample mean square deviation as the evaluation function of DWA:

$$f(C, \sigma, c_0) = \frac{1}{n} \sum_{i=1}^{n} \left| f(x_i) - y_i \right|, \tag{25}$$

where $f(x_i)$ and y_i denote the measured and expected values of the model, respectively. The optimization goal is to make $f(C, \sigma, c_0)$ reach the minimum value. n denotes the population number. The fitness function is $1/1 + f$. Parameter settings of the DWA algorithm are as follows: the evaluation number $Iter = 45$, the population size $N = 30$, differential variability factor $F = 0.75$, and crossover rate $CR = 0.9$. Compare DWA with GA (population size $N_1 = 30$, maximum generation $g_{\max} = 45$, replication

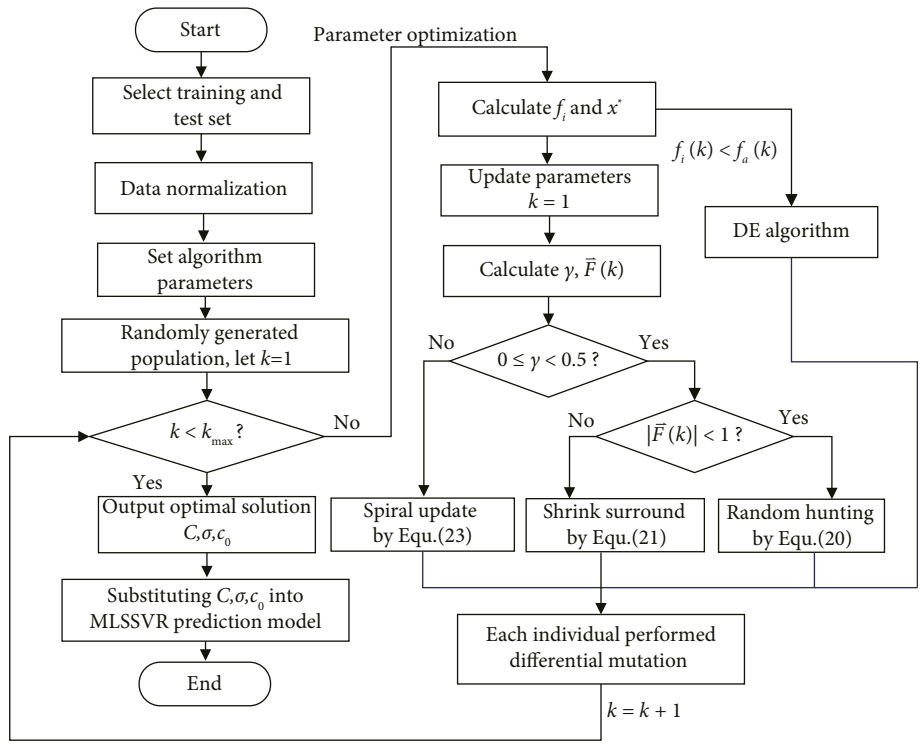

Figure 3: Work flow chart of the improved whale algorithm.

Table 1: Differential evolution whale algorithm.

Input: Population size; iterations; f_{obj}
Output: Optimal whale individual $x^*(k)$
1. Set whales population x_i, initial position $x_i(0)$, $k_{\max}$;
2. Calculate f_i of each whale according to f_{obj}
3. Update individual optimal location $x^*(k)$
4. while $(k \le k_{\max})$
5. for $i = 1$ to N do
6. Update parameter δ, $\vec{F}(k)$, $\vec{J}(k)$, $f_i(k)$ and γ;
7. if $(0 \le \gamma < 0.5)$
8. if $|\vec{F}(k)| < 1$
9. Update the location of the whale population by equation (20)
10. else if $|\vec{F}(k)| \ge 1$
11. Update the location of the whale population by equation (21)
12. end
13. else if $0.5 \le \gamma < 1$;
14. Update the location of the whale population by equation (23)
15. end
16. end
17. Calculate $f_i(k)$ and update $x_i^*(k)$;
18. if $f_i(k) < f_a(k)$
19. Update the individual position of whales by equation (24)
20. end
21. Let $k = k + 1$
22. end

probability $P_r = 0.65$, crossover probability $P_c = 0.85$, mutation probability $P_m = 0.05$), PSO (particle number $N_2 = 0.85$, maximum particle velocity $V_{\max} = 0.85$, acceleration constant $c_1 = c_2 = 2$), and GWA ($P_r = 0.7$, $P_c = 0.8$, $P_m = 0.01$), the parameter optimization curve is shown in Figure 4. The optimal parameters for MLSSVR prediction model using the DWA as follows: $C = 15.24.9$, $\sigma = 0.092$, and $c_0 = 9.74$.

The optimization results show that the improved whale optimization algorithm has a higher convergence accuracy and better stability than the other optimization algorithms and basic whale optimization algorithms.

6. Simulation Results and Analysis

To evaluate the accuracy of the parametric model of the coaxial cavity filter, the standard deviation (STD), the maximum absolute error (MAE), and the correlation coefficient (R) of three different methods are used for analysis and comparison. The calculation equation is as follows:

$$\text{STD} = \sqrt{\frac{1}{n-1}\sum_{i=1}^{n}\sum_{r=1}^{q}\left|f(x_{ir}) - \overline{y}_{ir}\right|^2},$$

$$\text{MAE} = \frac{1}{n}\sum_{i=1}^{n}\sum_{r=1}^{q}\left|f(x_{ir}) - y_{ir}\right|,$$

$$\text{R} = \frac{\sum_{i=1}^{n}\sum_{r=1}^{q}\left(f(x_{ir}) - \overline{f}(x_{ir})\right)\left(y_{ir} - \overline{y}_{ir}\right)}{\sqrt{\sum_{i=1}^{n}\sum_{r=1}^{q}\left(f(x_{ir}) - \overline{f}(x_{ir})\right)^2}\sqrt{\sum_{i=1}^{n}\sum_{r=1}^{q}\left(y_{ir} - \overline{y}_{ir}\right)^2}}, \tag{26}$$

where $f(x_{ir})$ and y_{ir} denote the real and predicted values of the measured data, respectively. n and q denote the number of samples and output variables, respectively. Substitute the

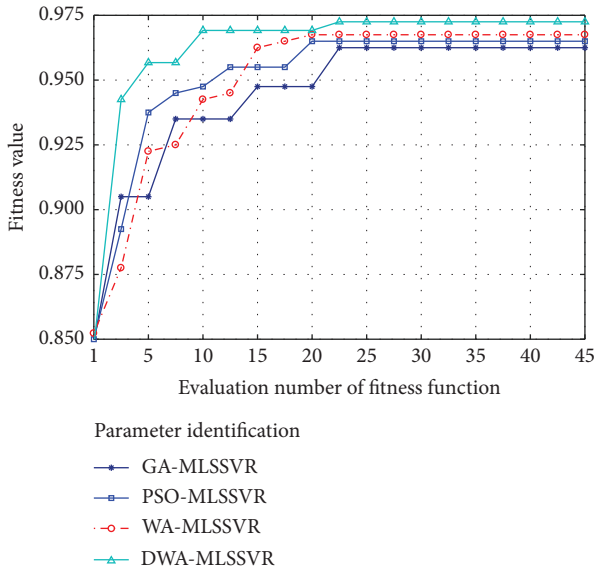

Figure 4: Fitness value for parameter identification of different algorithms.

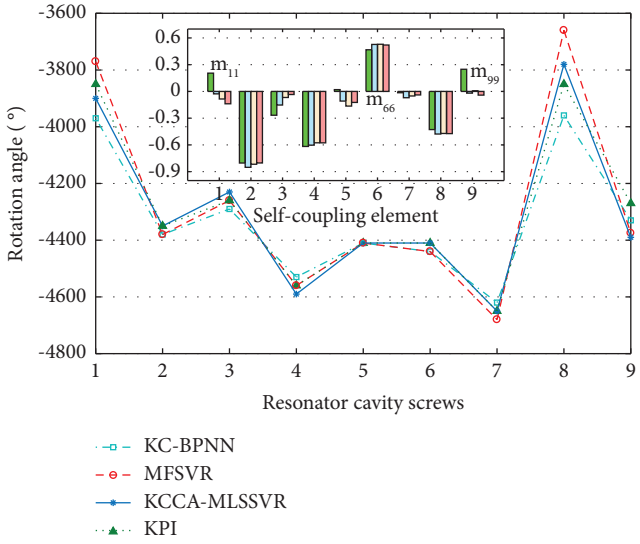

Figure 5: Tuning the screw rotation angle of the ninth-order cavity filter with different methods.

tuning process relationship data into the parameter prediction model, and compare the kernel clustering back propagation neural network (KC-BPNN) and multioutput fuzzy support vector regression (MFSVR) with the KCCA-MLSSVR method proposed in this paper. The prediction results are shown in Figures 5 and 6. It can be seen from this figure that the STD and MAE of the proposed method prediction results are lower than those of the other two models; in addition, the absolute value of R by the proposed model is close to 1, which is higher than the other two methods. The above results indicate that the proposed method can not only effectively reduce the impact of high-dimensional data on the model's prediction accuracy but also improve the model's adaptability and generalization

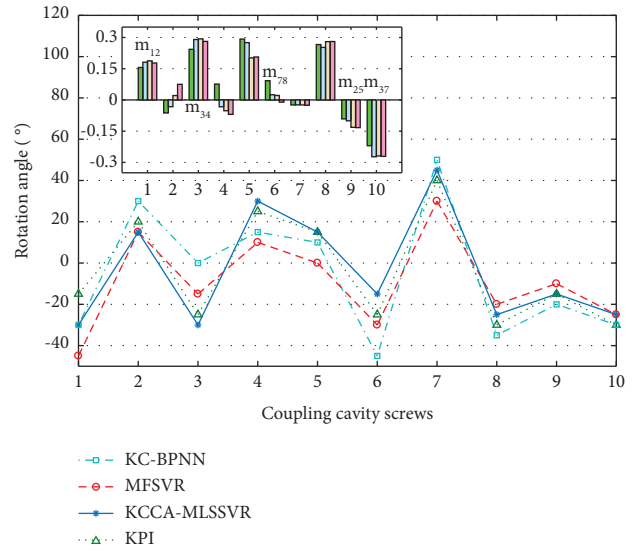

Figure 6: Coupling screws rotation angle of the ninth-order cavity filter with different methods.

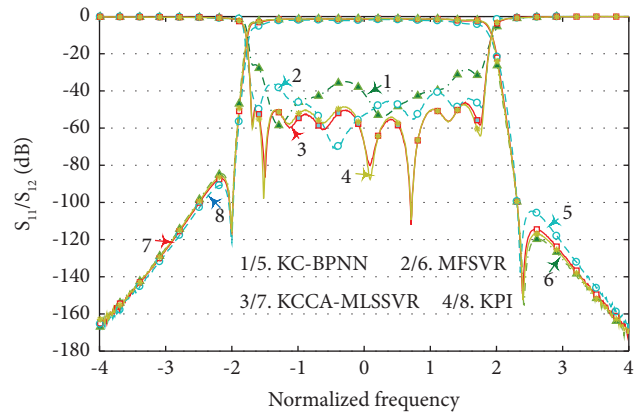

Figure 7: Output response curves of the ninth-order cavity filter with different methods.

ability. The S-parameter simulation curve of the ninth-order cavity filter with three different methods is shown in Figure 7.

The purpose of cavity filter tuning is to make the S-parameters of the output response meet the key performance indexes (KPI) required before production. To further verify the feasibility of the method, a ten-order cross-coupled cavity filter with complicated topology is taken as the experimental object for simulation experiments. Kpis are as follows: center frequency $f_0 = 2.38\text{GHz}$, passband width $bw = 0.10\text{GHz}$, the maximum return loss $RL = -34dB$, maximum insertion loss $IL = -0.35dB$. It can be seen from Figure 8 that the return loss, insertion loss, and out-of-band suppression of the proposed method can meet the KPI.

For more quantitative comparison, the insertion loss (IL), return loss (RL), and left and right out-of-band suppression (RS or LS) of S-parameters calculated by different methods are shown in Tables 2 and 3. From the data given in the table, the proposed method in this study is

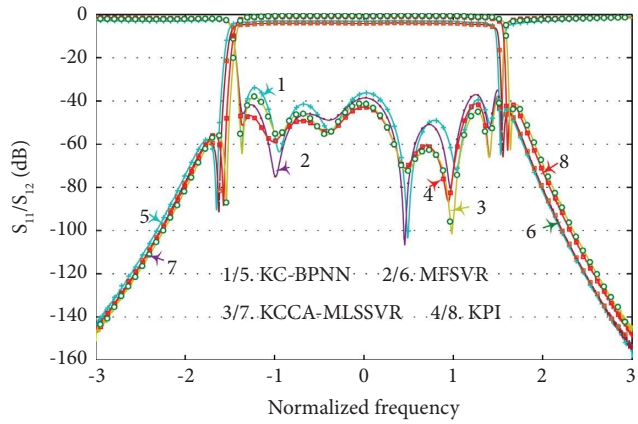

Figure 8: Output response curves of the eighth order cavity filter with different methods.

Table 2: Key performance indicators of different methods for ninth-order cavity filter.

Methods	IL_{max} (dB)	IL_{min} (dB)	RS (dB)	LS (dB)
KC-BPNN	−0.7390	−0.5216	−119.23	−91.17
LS-SVR	−0.9706	−0.5032	−104.71	−84.57
GPR	−0.8203	−0.4726	−116.15	−86.07
KCA-MLSSVR	−0.5654	−0.4013	−114.13	−86.02
KPI	−0.4315	−0.3074	−116.08	−85.34

Table 3: Key performance indicators of different methods for the tenth order cross-coupled filter.

Methods	IL_{max} (dB)	IL_{min} (dB)	RS (dB)	LS (dB)
KC-BPNN	−1.0204	−0.9612	−42.35	−58.05
LS-SVR	−0.9315	−0.6102	−41.71	−55.54
GPR	−0.8105	−0.5612	−42.74	−55.76
KCA-MLSSVR	−0.6317	−0.4426	−43.86	−56.32
KPI	−0.4175	−0.3702	−42.96	−55.76

consistent with the KPI, while the *S*-parameters using KC-BPNN, LS-SVR, and Gaussian process regression (GPR) methods have large deviation.

7. Conclusion

The tuning process of the coaxial cavity filter has great nonlinearity, and the output characteristics vary greatly in different tuning stages. To solve this problem, a parametric model method for coaxial cavity filter fusing KCCA and MLSSVR is proposed in this study. First, the redundant eigenvectors are digested by KCCA, which not only reduces the input vector dimension of the prediction model but also accelerates the training speed of the system. Second, a parametric model using MLSSVR has higher prediction accuracy than traditional modeling methods. Finally, the model parameters are optimized by DWA, which improves the adaptive ability and convergence speed of the model. The experimental results show that the proposed method in this study has higher prediction accuracy and generalization performance in the process of cavity filter model parameter fitting.

Data Availability

The data used to support the findings of this study are available from the corresponding author upon request.

Conflicts of Interest

The authors declare that they have no conflicts of interest.

Acknowledgments

This work is supported by the National Natural Science Foundation of China under grant 62141102, Jiangxi Provincial Natural Science Foundation under grant 20202BAB202008, Doctoral Science Research Foundation of East China University of Technology under grant DHBK2019178, and the Education Department Foundation of Jiangxi Province under grant GJJ2200726.

References

[1] J. J. Michalski, "Inverse modeling in application for sequential filter tuning," *Progress in Electromagnetics Research*, vol. 115, no. 2, pp. 113–129, 2011.

[2] H. Youssef, "Accurate modeling and optimization of microwave circuits and devices using adaptive neuro-fuzzy inference system," *International Journal of Microwave and Wireless Technologies*, vol. 3, no. 6, pp. 867–879, 2011.

[3] Y. Cao, S. Reitzinger, and Q. J. Zhang, "Simple and efficient high-dimensional parametric modeling for microwave cavity

filters using modular neural network," *IEEE Microwave and Wireless Components Letters*, vol. 21, no. 5, pp. 258–260, 2011.

[4] C. Zhang, J. Jin, W. C. Na, Q. J. Zhang, and M. Yu, "Multivalued neural network inverse modeling and applications to microwave filters," *IEEE Transactions on Microwave Theory and Techniques*, vol. 66, no. 8, pp. 3781–3797, 2018.

[5] V. Miraftab and R. R. Mansour, "Fully automated RF microwave filter tuning by extracting human experience using fuzzy controllers," *IEEE Transactions on Circuits and Systems I: Regular Papers*, vol. 55, no. 5, pp. 1357–1367, 2008.

[6] J. Z. Zhou, B. Duan, J. Huang, and H. J. Cao, "Data-driven modeling and optimization for cavity filters using linear programming support vector regression," *Neural Computing & Applications*, vol. 24, no. 7-8, pp. 1771–1783, 2014.

[7] J. Z. Zhou, J. Huang, P. Li, and N. Li, "Hybrid modeling of microwave devices using multi-kernel support vector regression with prior knowledge," *International Journal of RF and Microwave Computer-Aided Engineering*, vol. 25, no. 3, pp. 219–228, 2015.

[8] M. A. Alvarez, N. D. Lawrence, and E. Rasmussen, "Computationally efficient convolved multiple output Gaussian processes," *Journal of Machine Learning Research*, vol. 12, pp. 1459–1500, 2011.

[9] J. Zhao and S. L. Sun, "Variational dependent multi-output Gaussian process dynamical systems," *Journal of Machine Learning Research*, vol. 17, no. 121, pp. 1–36, 2016.

[10] L. Yang, K. Wang, and L. S. Mihaylova, "Online sparse multioutput Gaussian process regression and learning," *IEEE Transactions on Signal and Information Processing over Networks*, vol. 5, no. 2, pp. 258–272, 2019.

[11] D. Xu, Y. Shi, I. W. Tsang, Y. S. Ong, C. Gong, and X. Shen, "Survey on multi-output learning," *IEEE Transactions on Neural Networks and Learning Systems*, vol. 31, no. 7, pp. 2409–2429, 2020.

[12] D. Xu, Y. Shi, Tsang et al., "Joint estimation of target range and velocity for radar system via complex-valued kernel quasi-Newton method," *IEEE Transactions on Instrumentation and Measurement*, vol. 71, Article ID 8502413, 2022.

[13] Z. Wang, S. Jin, J. Yang, X. Wu, and Y. Ou, "Real-time tuning of cavity filters by learning from human experience: a vector field approach," in *Proceedings of the IEEE 12th World Congress on Intelligent Control and Automation*, pp. 1931–1936, Guilin, China, June 2016.

[14] S. Li, X. Fan, P. D. Laforge, and Q. S. Cheng, "Surrogate model-based space mapping in postfabrication bandpass filters' tuning," *IEEE Transactions on Microwave Theory and Techniques*, vol. 68, no. 6, pp. 2172–2182, 2020.

[15] W. Shengbiao, C. Weihua, L. Can, and W. Min, "A computer-aided tuning method for microwave filters by combing T-S fuzzy neural networks and improved space mapping," *Computer Modeling in Engineering and Sciences*, vol. 116, no. 3, pp. 433–453, 2018.

[16] G. Pan, Y. Wu, M. Yu, L. Fu, and H. Li, "Inverse modeling for filters using a regularized deep neural network approach," *IEEE Microwave and Wireless Components Letters*, vol. 30, no. 5, pp. 457–460, 2020.

[17] M. Mina, M. Rezaei, A. Sameni, Y. Ostovari, and C. Ritsema, "Predicting wind erosion rate using portable wind tunnel combined with machine learning algorithms in calcareous soils, southern Iran," *Journal of Environmental Management*, vol. 304, no. 304, pp. 114171–171, 2022.

[18] P. Duan, K. Xie, T. Guo, and X. Huang, "Short-term load forecasting for electric power systems using the PSO-SVR and FCM clustering techniques," *Energies*, vol. 4, no. 1, pp. 173–184, 2011.

[19] Y. L. Zeng, W. Chen, Z. B. Tang, and J. Wu, "Joint proportional task offloading and resource allocation for MEC in ultra-dense networks with improved whale optimization algorithm," *Journal of Physics: Conference Series*, vol. 1646, no. 1, pp. 1–7, 2020.

[20] W. H. Cao, C. Liu, Y. Yuan, and M. Wu, "Extracting coupling matrix from lossy filters with uneven-Qs using differential evolution optimization technique," *International Journal of RF and Microwave Computer-Aided Engineering*, vol. 28, no. 6, pp. e21269–e21814, 2018.

[21] Y. Zhang, K. L. Wu, and F. Seyfert, "A direct preconditioner for coupling matrix reconfiguration of bandpass filters with irregular couplings using continuation method," *IEEE Transactions on Microwave Theory and Techniques*, vol. 69, no. 2, pp. 1394–1403, 2021.

[22] Q. Chen and Y. Wang, "Key-performance-indicator-related state monitoring based on kernel canonical correlation analysis," *Control Engineering Practice*, vol. 107, pp. 104–116, Article ID 104692, 2021.

[23] W. Lei, K. Wei, and S. Q. Wu, "Detecting genetic associations with brain imaging phenotypes in Alzheimer's disease via a novel structured KCCA approach," *Journal of Bioinformatics and Computational Biology*, vol. 9, no. 4, pp. 215–224, 2021.

[24] Y. Zhao, H. Zhang, Y. Wang, C. Li, R. Xu, and C. Yang, "An extended binary subband canonical correlation analysis detection algorithm oriented to the radial contraction-expansion motion steady-state visual evoked paradigm," *Brain Science Advances*, vol. 8, no. 1, pp. 19–37, 2022.

[25] C. C. Chang and C. J. Lin, "Training v-support vector regression: theory and algorithms," *Neural Computation*, vol. 14, no. 8, pp. 1959–1977, 2002.

[26] N. Soleimani and R. Trinchero, "Compressed complex-valued least squares support vector machine regression for modeling of the frequency-domain responses of electromagnetic structures," *Electronics*, vol. 11, no. 4, pp. 551–562, 2022.

[27] K. Huang, M. Y. You, Y. X. Ye, B. Jiang, and A. N. Lu, "Direction of arrival based on the multioutput least squares support vector regression model," *Mathematical Problems in Engineering*, vol. 2020, no. 3, Article ID 8601376, 8 pages, 2020.

[28] Y. Sun and Y. Chen, "Multi-population improved whale optimization algorithm for high dimensional optimization," *Applied Soft Computing*, vol. 112, no. 2, p. 7, 2021.

[29] C. Sun, Y. Jin, C. Ran, J. Ding, and J. Zeng, "Surrogate-assisted cooperative swarm optimization of high-dimensional expensive problems," *IEEE Transactions on Evolutionary Computation*, vol. 99, pp. 1–12, 2017.

[30] J. Cheng, J. Xu, W. Chen, and B. Song, "Locating and sizing method of electric vehicle charging station based on Improved Whale Optimization Algorithm," *Energy Reports*, vol. 8, pp. 4386–4400, 2022.